

The electrical properties of Au/MEH-PPV:PCBM/n-type GaAs Schottky barrier diode

M. AHMETOGLU (AFRAILOV)^{a,*}, A. KIRSOY^a, A. ASİMOV^a, B. KUCUR^a

^aDepartment of Physics, Faculty of Sciences and Arts, Uludağ University, 16059 Gorukle, Bursa, Turkey

We fabricated the Au/MEH-PPV:PCBM/n-type GaAs Schottky barrier diodes (SBDs). Then we investigated Current-voltage (I-V) and capacitance-voltage (C-V) characteristics of the diode at room temperature. MEH-PPV:PCBM (in a mass ratio 1:4) used as interfacial layer between metal and semiconductor layers. Here, MEH-PPV is poly [2-methoxy-5-(ethylhexyloxy)-1,4-phenylenevinylene] and PCBM is [6,6]-phenyl-61C-butric acid methyl ester). SBD parameters such as ideality factor, barrier height and series resistance were obtained from I-V and C-V measurements. Also, Cheung functions and Norde Method were used to evaluate the I-V characteristics and to determine the characteristic parameters of the Schottky diode. The diode parameters such as ideality factor, barrier heights and series resistance were found as 4.39-4.54 and 0.57-0.63 eV and 51-53 Ω respectively. Also the interface states energy distribution of the diode was determined and found as $1.09 \times 10^{12} \text{ eV}^{-1} \text{ cm}^{-2}$ at (Ec-0.352) eV to $2.94 \times 10^{11} \text{ eV}^{-1} \text{ cm}^{-2}$ at (Ec-0.436) eV.

(Received December 12, 2014; accepted November 25, 2016)

Keywords: Schottky barrier diode, Series resistance, Ideality factor, Conducting polymers

1. Introduction

The metal-semiconductor junction is more commonly known as the Schottky barrier diode. Metal-semiconductor structures are used as a basic component for the performance of semiconductor devices due to their potential application in many electronic and optoelectronic devices. Schottky barrier diode are widely used in very important applications in electronic industry, such as microwave mixer, high-current power supplies, solarcell, photodetector, field-effect transistors (FETs) etc. [1-3].

Conjugated polymers are recognized as organic semiconductors with electronic properties and they have found a wide application area in electronic technology [8].

It is well known that the electrical characteristics of a Schottky diode are controlled mainly by its interface properties [4]. In order to obtain desired characteristics for diode applications, the electrical properties of metal/semiconductor (MS) structures can be modified by introducing organic layer on semiconductor materials [9,10].

Over the recent decades, there have been significant advances in the scientific domain with regard to electronic devices that are based upon organic components, mainly due to they have a number of advantages such as easy and low cost device fabrication, versatility of usage, and large area coverage [5-16].

Recently, heterojunction devices, which include an organic material as an active layer, have become very famous and popular to provide low operating voltage for low power nanoscale devices due to easy fabrication process as a very thin layer. MEH-PPV and PCBM are quite attractive and good candidates as a p-type and n-type layer respectively [8,17].

PPV in itself is a very intractable material due to its insolubility. Adding alkyl or alkoxy chains on the phenylene rings, as in MEH- and MDMO-PPV, makes these materials processable and soluble in some organic solvents such as chloroform, chlorobenzene, or 1,2-dichlorobenzene (ODCB). The dialkoxy side groups also modify the polymer's bandgap, so that the emission color bathochromically shifts to orange from the yellow-green of the unsubstituted PPV. MEH-PPV is good soluble in various organic solvents, easy to manufacture and has the properties as being oxidation resistant a conductive polymer. Because of these properties has a wide range of applications [18,19].

PCBM has shown to be broadly applicable as solution processable organic n-type semiconductors. The variations available represent opportunities for optimization in various devices. The blended PCBM with appropriate conjugated polymers can be used in the photovoltaic cells production, thin film organic field effect transistor (OFET) fabricated and photodetector production. PCBM is dissolved in the same solvent with p-type semiconductors MEH-PPV, MDMO-PPV and P3HT [20].

MEH-PPV and PCBM have LUMO/HOMO values respectively 3 eV /5.3 eV and 3.75 eV /6.1 eV [21,22].

In this study, MEH-PPV:PCBM (1:4 by mass ratio) thin interfacial polymer layer was deposited on n-GaAs using spin coating system to obtain as a new structure Au/n-GaAs/MEH-PPV:PCBM/Al Schottky barrier diode. The electronic parameters of the diode were determined by using current – voltage and capacitance – voltage measurements at room temperature.

2. Experimental procedures

Au/n-GaAs/MEH-PPV:PCBM/Al Schottky barrier diode was fabricated on n-type GaAs semiconductor wafer with (100) orientation, 400 μm thickness and 50.8 mm diameter. Firstly, the wafer was chemically cleaned using the RCA cleaning procedure (i.e. 10 min boil in $\text{H}_2\text{SO}_4 + \text{H}_2\text{O}_2$ followed by a 10 min $\text{HCl} + \text{H}_2\text{O}_2 + 6\text{H}_2\text{O}$ at 60 $^\circ\text{C}$). It was immersed in diluted 20% HF for 60 s. The wafer was rinsed in de-ionized water of resistivity 18 $\text{M}\Omega\text{ cm}$ with ultrasonic cleaning in each step. After that, the sample was dried in the high-purity nitrogen stream and inserted into the deposition chamber. Au (99.99%) and Ge (99.99%) were used for ohmic contact [1]. The ohmic contact with a thickness of $\sim 1875 \text{ \AA}$ was made by evaporating 99.99% purity Au metal and germanium on the back of the surface wafer in a thermal evaporator unit at 10^{-6} Torr. Then it was annealed at 450 $^\circ\text{C}$ for 5 min in flowing N_2 in a quartz tube furnace. Front surface of samples were coated with a conducting polymer MEH-PPV:PCBM (with a mass ratio of 1:4) (Fig. 1) [16] film by spin coating (VTC-100) with 1200 rpm for 60 s. After that rectifier Schottky contacts were formed on the other faces by evaporating $\sim 1000 \text{ \AA}$ thickness and 99.99% purity Al. All evaporation processes were carried out in a vacuum coating unit at about 5.1×10^{-6} Torr. Thus, Au/n-GaAs/MEH-PPV:PCBM/Al sandwich Schottky barrier type diode was fabricated.

The I–V measurements were performed using a Keithley 6517A electrometer and C–V measurements were carried out at room temperature with a Keithley HP-4194 C–V Analyzer. All measurements were controlled by a computer via an IEEE–488 standard interface so that the data collecting, processing and plotting could be accomplished automatically.

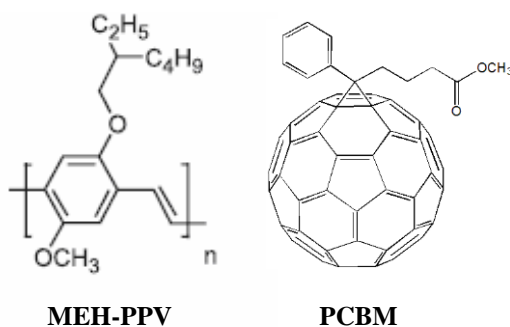


Fig. 1. Molecular structure of MEH-PPV and PCBM

3. Results and discussion

The semi-logarithmic current–voltage (I–V) curve of the device is shown in Fig. 2 at room temperature. According to the thermionic emission theory the current–voltage characteristics of a Schottky diode can be expressed by the following relation: [24,25]

$$I = I_0 \exp\left(\frac{qV}{nkT}\right) \left[1 - \exp\left(-\frac{qV}{kT}\right)\right] \quad (1)$$

where I is the measured current, V is the applied bias voltage, n is the ideality factor, k is the Boltzmann's constant, T is the temperature in Kelvin, q is the electronic charge and I_0 is saturation current derived from the straight line intercept of $\ln I$ - V plot at zero bias, and is given by

$$I_0 = AA^*T^2 \exp\left(-\frac{q\Phi_{b0}}{kT}\right) \quad (2)$$

where A is the rectifier contact area, A^* is the Richardson constant and equals to $8.16 \text{ A cm}^{-2}\text{K}^{-2}$ for n-type GaAs [2,26] and Φ_{b0} (I–V) is the zero bias barrier height. From Eq.(1), ideality factor n can be written as

$$n = \frac{q}{kT} \left(\frac{dV}{d(\ln I)} \right) \quad (3)$$

n equals to one for an ideal diode. However, n has usually a value greater than unity. High values of n can be attributed to the presence of the interfacial layer, barrier height inhomogeneity or image-force lowering which is voltage dependent [1,25]. Φ_{b0} is the zero-bias barrier height (BH), which can be extracted from Eq.(2) and it can be written as

$$\Phi_{b0} = \frac{kT}{q} \ln\left(\frac{AA^*T^2}{I_0}\right) \quad (4)$$

The semilog-forward and reverse bias I–V characteristics of the Au/MEH-PPV:PCBM/n-GaAs/Al structure at room temperature are given in Fig. 2. The values of the barrier height and ideality factor were found as $\Phi_{b0} = 0.57 \text{ eV}$ from the experimental saturation current I_0 , and $n = 4.39$ from the slope of the linear region of the semilog-forward bias I–V characteristics indicating that the effect of series resistance in this region was not important, by using Eqs. (3) and (4) respectively. For an ideal Schottky barrier diode $n = 1$. Our n ideality factor value is considerably larger and in agreement with literature for these structures. The high values in the ideality factor are caused possibly by various effects such as inhomogeneities of MEH-PPV:PCBM film thickness, non-uniformity of the interfacial charges and series resistance [1,4,25].

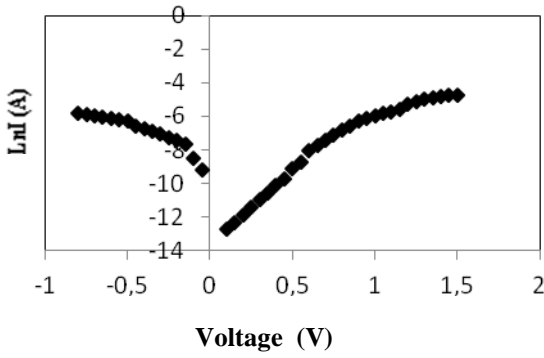


Fig. 2. Current versus voltage characteristic of the Au/n-GaAs/MEH-PPV:PCBM/Al at room temperatures

The forward bias I-V characteristics of the rectifying contacts might be deviated considerably from ideal behaviour due to the certain factors related with increasing voltage. These factors are the interface state density and the series resistance (R_s). The effect of series resistance is attributed to the presence of the interface layer between the metal and the semiconductor and leads to non-linearity [3,23,27]. The series resistance R_s is an important parameter, affecting the electrical characteristics of Schottky barrier contacts. The Schottky diode parameters such as the barrier height, the ideality factor and the series resistance can also be obtained using a method developed by Cheung at al. [28]. The values of the series resistance can be determined by following functions:

$$\frac{dV}{d(\ln I)} = IR_s + n\left(\frac{kT}{q}\right) \quad (5)$$

$$H(I) = V - n\left(\frac{kT}{q}\right) \ln\left(\frac{I}{AA * T^2}\right) \quad (6)$$

and $H(I)$ is given as follows:

$$H(I) = IR_s + n\Phi_{b0} \quad (7)$$

where R_s is the series resistance.

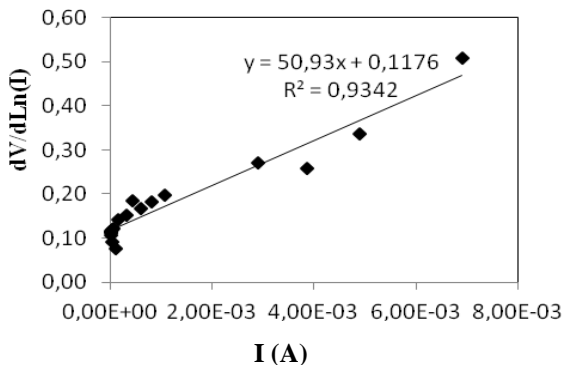


Fig. 3. Plot of $dV / d \ln I$ versus I for the Au/n-GaAs/MEH-PPV:PCBM/Al diode at room temperature

The plot of $dV/d(\ln I)$ versus I is shown in Fig. 3. The n and R_s values were calculated from the slope and intercept of $dV/d(\ln I)$ versus I plot and were found to be 4.54 and 51 Ω , respectively. The ideality factor obtained from $dV/d(\ln I)$ - I plot is seen to be greater than that obtained from $\ln I$ - V characteristic. The difference between the values of the ideality factors can be attributed to the fact that the first one is only under the effect of the interfacial properties and the second one is under the effect of both the interfacial properties and the series resistance [5,10].

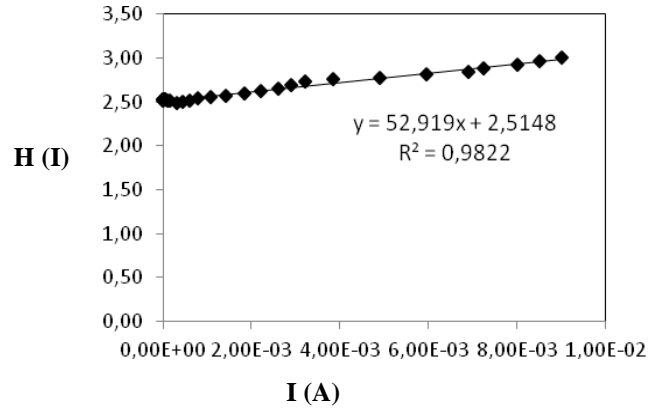


Fig. 4. Plot of $H(I)$ versus I for the Au/n-GaAs/MEH-PPV:PCBM/Al diode at room temperature

The plot of $H(I)$ versus I is shown in Fig. 4. The R_s and Φ_{b0} values were calculated from the slope and intercept of $H(I)$ versus I plot and were found to be 53 Ω and 0.57 eV, respectively. It can be seen clearly that the value of R_s obtained from $dV/d(\ln I)$ - I plot is in agreement with value obtained from $H(I)$ - I plot. This shows a good consistency with each other the values of series resistance obtained by applying Cheung's functions.

Alternatively, the values of barrier height and series resistance of the device have been obtained from Norde's functions [6,29]. The Norde function is given as

$$F(V) = \frac{V}{\gamma} - \left(\frac{kT}{q}\right) \ln\left(\frac{I(V)}{AA * T^2}\right) \quad (8)$$

where γ is a dimensionless integer with a value greater than ideality factor. That is, according to our results, the value of γ is 5. The $I(V)$ is the value of current taken from the I-V curve. If the minimum of the $F(V)$ versus V plot is determined, then the value of barrier height can be calculated by using following equation;

$$\Phi_b = F(V_0) + \frac{V_0}{\gamma} - \frac{kT}{q} \quad (9)$$

where $F(V_0)$ is the minimum point of $F(V)$, and V_0 is the corresponding voltage. The Norde plot for device is shown in Fig. 5.

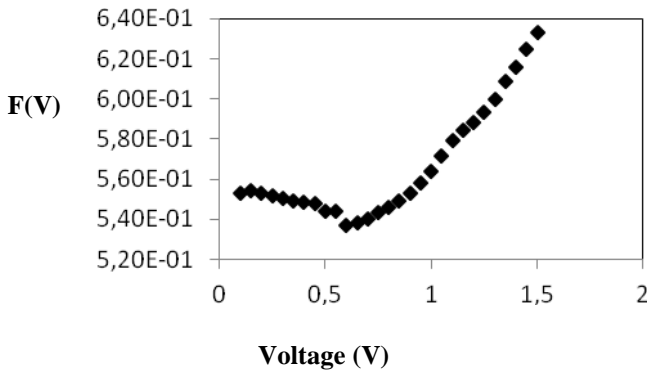


Fig. 5. $F(V)$ versus V plot of the Au/n-GaAs/MEH-PPV:PCBM/Al Schottky diode

The value of the series resistance has been calculated from Nord's function for device by using following relation:

$$R_s = \frac{kT(\gamma - n)}{qI_0} \quad (10)$$

According to Eq.(9) the value of barrier height were calculated as 0.63 eV by using $V_0 = 0.6$ V and $F(V_0) = 0.537$ eV. The values of series resistance were calculated as 50,92 Ω by using Eq.(10). The value of the series resistance obtained from Norde functions is lower than the values obtained from Cheung's function. Because the Cheung's functions are only applied to the nonlinear region (high voltage region) of the forward bias I-V characteristics while Norde's function is applied to the full forward bias I-V characteristics of the diode. In the high voltage region the slopes of the I-V characteristics are lower than those of the low voltage region. It is seen that there is an agreement between the values of the series resistance obtained from Cheung and Norde plots. There is a difference in the values of Φ_{b0} obtained from the forward-bias $\ln I-V$, Cheung functions and Norde functions. The discrepancy between different methods may result from such causes as contamination in the interface, an intervening insulating layer, edge leakage current, or deep impurity levels [25].

The analysis of the C-V measurements technique can be used to give information about the barrier parameters [4]. Thus, C-V measurements of the device were carried out at room temperature and 100 kHz with a Keithley HP-4194 C-V Analyzer. Fig. 6(a) shows the C - V characteristics and (b) reverse bias $C^{-2} - V$ characteristics of the device.

As can be seen in Fig. 6(a) that the values of the capacitance in reverse bias is slightly increasing towards low positive voltages and it is sharply increasing in forward bias towards high voltages. Fig. 6(b) shows the $C^{-2} - V$ characteristics of the diodes. It can be seen that the plot is linear.

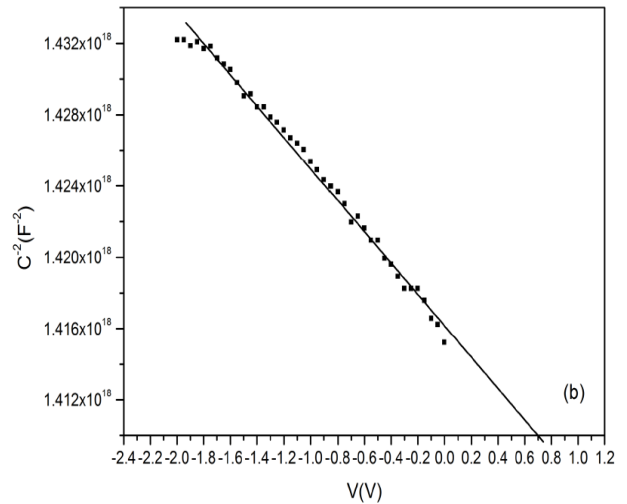
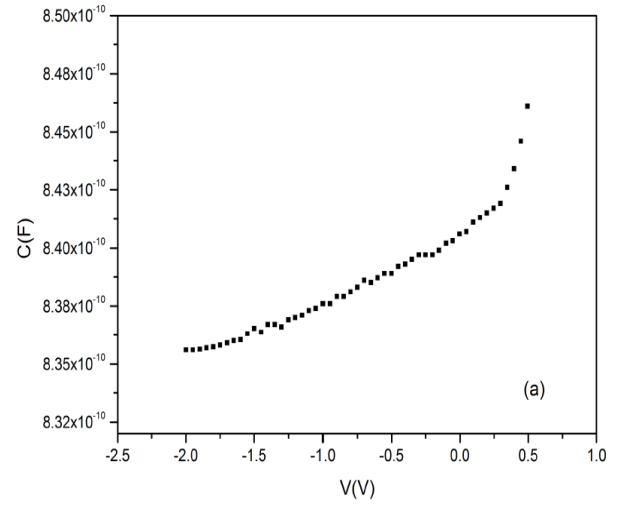


Fig. 6. (a) Plots of the experimental capacitance - voltage, and (b) reverse bias $C^{-2} - V$ characteristics of the Au/n-GaAs/MEH-PPV:PCBM/Al Schottky barrier diode in the frequency 100 kHz at room temperatures

The C - V characteristics of the diode can be analyzed by the following relation [1,13].

$$\frac{1}{C^2} = \frac{2(V_0 + V_r)}{q\epsilon_s A^2 N_D} \quad (11)$$

The slope of the reverse bias $C^{-2} - V$ plot can be also given by;

$$\frac{dC^{-2}}{dV} = \frac{2}{q\epsilon_s A^2 N_D} \quad (12)$$

Where V_r is the reverse bias voltage, V_0 is the built in potential at zero bias and is determined from the extrapolation of the $1/C^2 - V$ plot to the V -axis, ϵ_s is the dielectric constant of GaAs ($\epsilon_s = 13.1\epsilon_0$), [26] q is the

electronic charge and N_D is the doping concentration. According to Eq. (12), the doping concentration is determined to be $2.13 \times 10^{19} \text{ cm}^{-3}$ from the slope of the reverse bias $C^2 - V$ characteristics. The depletion width (W_d) and the value of the Fermi energy level (E_F) were calculated using following relations [1,2,13]:

$$W_d = \sqrt{\frac{2\epsilon_0\epsilon_s V_d}{qN_D}} \quad (13)$$

$$V_d = V_0 + \frac{kT}{q} \quad (14)$$

The Fermi energy level (E_F) is given by;

$$E_F = \frac{kT}{q} \ln\left(\frac{N_C}{N_D}\right) \quad (15)$$

and the effective density of states (N_C) in the GaAs conduction band is

$$N_C = \left[\frac{2\pi m_e^* k_B T}{h^2} \right]^{3/2} \quad (16)$$

Where $m_e^* = 0.067m_0$ is the effective mass the electron [2], and m_0 is the rest mass of the electron. V_0 is determined as 0.7 V from the extrapolation of the $1/C^2 - V$ plot to the V -axis. Thus, according to Eq. (14) V_d is calculated as 0.725 V and according to Eq.(13) W_d is calculated as 6.77×10^{-7} cm. Barrier height $\Phi_b(C-V)$ can be calculated using following relation:

$$\Phi_b(C-V) = V_d + E_F \quad (17)$$

Thus, $\Phi_b(C-V)$ were calculated 0.63 eV.

As we can be seen from the $C - V$ measurements obtained barrier height value is higher than from the $I-V$ measurements. This discrepancy is possibly resulted from the existence of interfacial MEH-PPV:PCBM layer and the barrier inhomogeneities [25].

The determination of the interface state density is important for the information about the quality of the structure. Because the interface state density affects the electronic parameters of the diode. Therefore we investigated interface state density. The density of the interface state of the diode can be obtained from the forward bias $I-V$ characteristics at room temperature by the following relation: [30]

$$n(V) = 1 + \frac{\delta}{\epsilon_i} \left(\frac{\epsilon_s}{W_d} + qN_{ss} \right) \quad (18)$$

Thus, according to Eq.(18), the interface state density can be obtained as below:

$$N_{ss}(V) = \frac{1}{q} \left\{ \frac{\epsilon_i}{\delta} [n(V) - 1] - \frac{\epsilon_s}{W_d} \right\} \quad (19)$$

Where W_d is the depletion width, δ is the thickness of the interfacial layer, N_{ss} is the density of the interface states, $\epsilon_s(13.1\epsilon_0)$ [26] and $\epsilon_i(3\epsilon_0)$ [17] are the permittivity of the semiconductor and interfacial layer, respectively. In n-type semiconductors, the energy of the interface states with respect to the bottom of the conduction band at the surface of the semiconductor is given by [31],

$$E_c - E_{ss} = q(\Phi_e - V) \quad (20)$$

Where V is the applied drop across the depletion layer and Φ_e is the effective barrier height and E_{ss} is the energy corresponding to the bottom of the conduction band at the surface of the semiconductor. The relationship between effective barrier height, applied voltage V and the ideality factor n is given by

$$\Phi_e = \Phi_{b0} + \left(1 - \frac{1}{n}\right)V \quad (21)$$

Thus, the energy distribution profile of N_{ss} as a function ($E_c - E_{ss}$) for Au/n-GaAs/MEH-PPV:PCBM/Al was obtained from the forward bias $I-V$ measurements by taking the bias dependence of the effective barrier height (Φ_e) into account by using Eq. (19), (20) and (21). The interface state density versus ($E_c - E_{ss}$) curve of the diode is given in Fig. 7. As can be seen from Fig. 7, the interface states density was calculated varied from $1.09 \times 10^{12} \text{ cm}^{-2}\text{eV}^{-1}$ in ($E_c - 0.352$) eV to $2.94 \times 10^{11} \text{ cm}^{-2}\text{eV}^{-1}$ in ($E_c - 0.436$) eV. That is, there is an exponential decrease from bottom of conduction band towards to midgap of GaAs. This confirms that the density of interface states changes with applied bias and each of applied biases corresponds to a different position in the GaAs band gap.

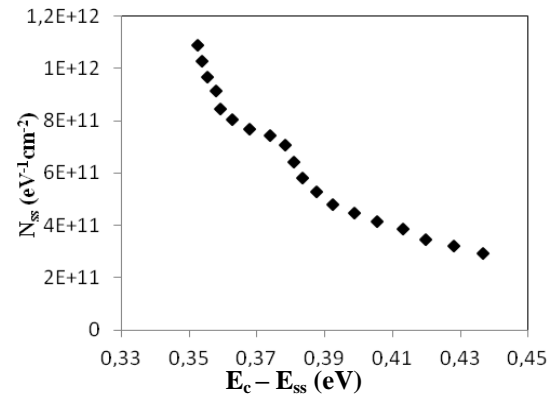


Fig. 7. Energy distribution of interface state density of the Au/n-GaAs/MEH-PPV:PCBM/Al Schottky diode

4. Conclusion

In this study, we fabricated Au/n-GaAs/MEH-PPV:PCBM/Al Schottky diode as a new structure. The electrical properties of the diode have been investigated at room temperature by using current – voltage and capacitance - voltage methods. The diode parameters such as ideality factor, barrier heights and series resistance were found as 4.39-4.54 and 0.57-0.63 eV and 51-53 Ω respectively, by using forward bias I-V, Cheung's functions and Norde method. There is a good agreement with the values of series resistance obtained from Cheung's functions and Norde's functions. The barrier height was also calculated from C-V measurements as 0.63 eV and this value is higher than from I-V measurement. This discrepancy is possibly resulted from the the existence of interfacial MEH-PPV:PCBM layer and the barrier inhomogeneities.

This diode showed a rectifying behavior and yielded different barrier height and ideality factor in comparison to conventional GaAs diode. The control of the electronic properties of the diode was accomplished by using thin interlayer of the MEH-PPV:PCBM. Also, the energy of interface states were determined from the forward bias I-V measurements by taking the bias dependence of the effective barrier height (Φ_e) into account. The interface state density decreases exponentially with bias from $1.09 \times 10^{12} \text{ cm}^{-2} \text{ eV}^{-1}$ in $(E_c - 0.352) \text{ eV}$ to $2.94 \times 10^{11} \text{ cm}^{-2} \text{ eV}^{-1}$ in $(E_c - 0.436) \text{ eV}$.

References

- [1] K. Ng. Kwok, Complete Guide To Semiconductor Devices, McGraw-Hill, Inc., New York, (1995).
- [2] J. Singh, Semiconductor Optoelectronics Physics and Technology, McGraw, Hill Inc., New York, (1995).
- [3] M. Soylu, O. A. Al-Hartomy, S. A. F. Al Said, A. A. Al-Ghamdi, I. S. Yahia, F. Yakuphanoglu, Microelectronics Reliability **53**, 1901 (2013).
- [4] E. H. Rhoderick, R. H. Williams, Metal–Semiconductor Contacts, Clarendon, Oxford, (1988).
- [5] A. Asimov, M. Ahmetoglu (Afrailov), Optoelectron. Adv. Mat. **8**, 975 (2014).
- [6] M. E. Aydın, M. Soylu, F. Yakuphanoglu, W. A. Farooq, Microelectronic Engineering **88**, 867 (2011).
- [7] A. Böhler, P. Urbach, J. Schöbel, S. Dirr, H. H. Johannes, S. Wiese, D. Ammermann, W. Kowalsky, Physica E **2**, 562 (1998).
- [8] A. S. Kavasoglu, F. Yakuphanoglu, N. Kavasoglu, O. Pakma, Ö. Birgi, Ş. Oktik, Journal of Alloys and Compounds **492**, 421 (2010).
- [9] S. Zeyrek, E. Acaroglu, S. Altındal, S. Birdogan, M. M. Bülbül, Current Applied Physics **13**, 1225 (2013).
- [10] S. Sönmezoglu, S. Senkul, R. Taş, G. Çankaya, M. Can, Solid State Sciences **12**, 706 (2010).
- [11] F. Yakuphanoglu, M. Shah, W. A. Farooq, Acta Physica Polonica A **120**, 558 (2010).
- [12] M. E. Aydın, F. Yakuphanoglu, J. H. Eom, D. H. Hwang, Physica B **387**, 239 (2007).
- [13] S. Demirezen, Z. Sönmez, U. Aydemir, Ş. Altındal, Current Applied Physics **12**, 266 (2012).
- [14] H. G. Çetinkaya, H. Tecimer, H. Uslu, Ş. Altındal, Current Applied Physics **13**, 1150 (2013).
- [15] A. Gümüş, Ş. Altındal, Materials Science in Semiconductor Processing **28**, 66 (2014).
- [16] F. C. Krebs, J. E. Carle, N. C. Bagger, M. Andersen, M. R. Lilliedal, M. A. Hammond, S. Hvidt, Solar Energy&Solar Cells **86**, 499 (2005).
- [17] B. Minnaert, M. Burgelman, Proceeding of NUMOS, University of Gent, Electronics and Information Systems, Gent, Belgium 327 (2007)
- [18] F. C. Krebs, Polymer Photovoltaics a Practical Approach, SPIE Press, Bellingham, Washington, (2008).
- [19] Q. Pei. Material Matters **2**, 26 (2007).
- [20] D. Kronholm, J. C. Hummelen, Material Matters **2**, 16 (2007).
- [21] M. A. Ibrahim, A. K. Roth, U. Zhokhavets, G. Gobsch, S. Sensfuss, Solar Energy Materials & Solar Cells **85**, 13 (2005).
- [22] N. Mustapha, Z. Fekkai, A. Alkaoud, Optik **127**, 2755 (2016).
- [23] A. Asimov, M. Ahmetoglu (Afrailov), B. Kucur, M. Özer, T. Güzel, Optoelectron. Adv. Mat. **7**, 490 (2013).
- [24] K. S. Dieter, Semiconductor Material and Device Characterization, Wiley, New York, (1990).
- [25] S. M. Sze, Physics of Semiconductor Devices 2nd ed., Wiley, New York, (1981).
- [26] Ş. Karataş, A. Türüt, Physica B **381**, 199 (2006).
- [27] A. Türüt, M. Sağlam, H. Efeoğlu, N. Yalçın, M. Yıldırım, B. Abay, Physica B **205**, 41 (1995).
- [28] S. K. Cheung, N. K. Cheung, Appl. Phys. Lett. **49**, 85 (1986).
- [29] H. Norde, J. Appl. Phys. **50**, 5052 (1979).
- [30] H. C. Card, E. H. Rhoderick, J. Phys. D: Appl. Phys. **4**, 1589 (1971).
- [31] M. K. Hudait, S. B. Kruppanidhi, Solid State Electronics **44**, 1089 (2000).